Proceedings of ISAP2012, Nagoya, Japan

POS2-29

A Consideration of Performance Improvement of Location Estimation of Scatterers in MIMO Radar

#Tatsuya Hayashi, Nobuyoshi Kikuma,
Hiroshi Hirayama and Kunio Sakakibara
Department of Computer Science and Engineering, Nagoya Institute of Technology
Gokiso-cho, Showa-ku, Nagoya, 466-8555, Japan, kikuma@m.ieice.org

1. Introduction

In recent years, the frequency resource has been increasingly restricted by development of the mobile communications which have the multifunctional portable cellular phones etc. as typical products [1]. In that background, the technology which uses multiple antennas for both transmitting and receiving, called MIMO (Multiple-Input Multiple-Output), is proposed and widely used in the systems such as the wireless LAN. Similarly, in the radars, the MIMO technology is used and it is called MIMO radar. It is also uses multiple antennas to transmit and receive the signals, and thus provides high-resolution spatial spectrum estimates [2].

In this paper, we perform a location estimation of scatterers using the MIMO radar. Specifically, we introduce into the MIMO radar the MUSIC algorithm [1] which is the representative of nulling methods. In addition, we compare the performances between the MUSIC-based method and the conventional beamforming methods in the location estimation of scatterers, and clarify the performance difference between them.

2. Analysis Model of MIMO Radar

Consider a MIMO radar system with M_t-element transmitting uniform linear array and M_r-element receiving uniform liner array as shown in Fig.1. The transmitting and the receiving arrays are arranged in an identical line. The first elements of the transmitting array and the receiving array are used as the reference antenna, respectively, and the distance between the reference antennas is apart by δ. The system simultaneously transmits M_t linearly independent waveforms, denoted by $\boldsymbol{x}(n) \in C^{M_t \times 1}$ $(n = 1, \cdots, N)$ with N being the data sample number. Then, the transmitted data matrix denoted by $\boldsymbol{X} \in C^{M_t \times N}$ can be represented by

$$\boldsymbol{X} = [\boldsymbol{x}(1), \cdots, \boldsymbol{x}(N)] \quad (1)$$

Assuming that there are L point-scatterers (targets) with ranges R_l $(l = 1, \cdots, L)$ in the same range bin from the array axis, the received data matrix $\boldsymbol{Y} \in C^{M_r \times N}$ can be expressed as

$$\boldsymbol{Y} = [\boldsymbol{y}(1), \cdots, \boldsymbol{y}(N)] = \boldsymbol{B}\boldsymbol{\beta}\boldsymbol{A}^T\boldsymbol{X} + \boldsymbol{Z} = \boldsymbol{H}\boldsymbol{X} + \boldsymbol{Z} \quad (2)$$

$$\boldsymbol{A} = [\boldsymbol{a}(R_1, \theta_{t,1}), \boldsymbol{a}(R_2, \theta_{t,2}), \cdots, \boldsymbol{a}(R_L, \theta_{t,L})] \quad (3)$$

$$\boldsymbol{B} = [\boldsymbol{b}(R_1, \theta_{r,1}), \boldsymbol{b}(R_2, \theta_{r,2}), \cdots, \boldsymbol{b}(R_L, \theta_{r,L})] \quad (4)$$

$$\boldsymbol{a}(R_l, \theta_{t,l}) = \Big[\frac{r_{t1,l}}{r_{t1,l}} e^{-j2\pi\tau_{t1,l}}, \frac{r_{t1,l}}{r_{t2,l}} e^{-j2\pi\tau_{t2,l}}, \cdots, \frac{r_{t1,l}}{r_{tM_t,l}} e^{-j2\pi\tau_{tM_t,l}}\Big]^T \quad (5)$$

$$\boldsymbol{b}(R_l, \theta_{r,l}) = \Big[\frac{r_{r1,l}}{r_{r1,l}} e^{-j2\pi\tau_{r1,l}}, \frac{r_{r1,l}}{r_{r2,l}} e^{-j2\pi\tau_{r2,l}}, \cdots, \frac{r_{r1,l}}{r_{rM_r,l}} e^{-j2\pi\tau_{rM_r,l}}\Big]^T \quad (6)$$

$$\boldsymbol{H} = \boldsymbol{B}\boldsymbol{\beta}\boldsymbol{A}^T \quad (7)$$

$$\boldsymbol{\beta} = \mathrm{diag}\{\beta_1, \beta_2, \cdots, \beta_L\} \quad (8)$$

where $\boldsymbol{y}(n)$ is the nth received data sample, $\boldsymbol{a}(R_l, \theta_{t,l})$ and $\boldsymbol{b}(R_l, \theta_{r,l})$ are the spherical wave steering vectors of the transmitting and receiving arrays, respectively, $\boldsymbol{A} \in C^{M_t \times L}$ and $\boldsymbol{B} \in C^{M_r \times L}$ are the steering matrices of the transmitting and receiving arrays, respectively. Also, $[r_{t1,l}, \cdots, r_{tM_t,l}]$ and $[r_{r1,l}, \cdots, r_{rM_r,l}]$

represent the distances from each element of transmitting and receiving arrays to the lth target and $[\tau_{t1,l}, \cdots, \tau_{tM_t,l}]$ and $[\tau_{r1,l}, \cdots, \tau_{rM_r,l}]$ represent the time lags from each elements to the lth target relative to the reference antenna of each array. In addition, $\theta_{t,l}$ is the angle of the lth target from the broadside direction at the reference antenna element of the transmitting array(called transmission angle), and similarly $\theta_{r,l}$ is the angle of the lth target from the broadside direction at the reference antenna element of the receiving array (called reception angle). $\boldsymbol{\beta}$ is the complex amplitude matrix corresponding to the reflection coefficient of the targets, $\boldsymbol{H}$ is the channel response matrix representing the propagation path information, and $\boldsymbol{Z} \in C^{M_r \times N}$ denotes the noise term, which includes interferences from targets other than L targets and at other range bins. Also, $(\cdot)^T$ denotes the transpose.

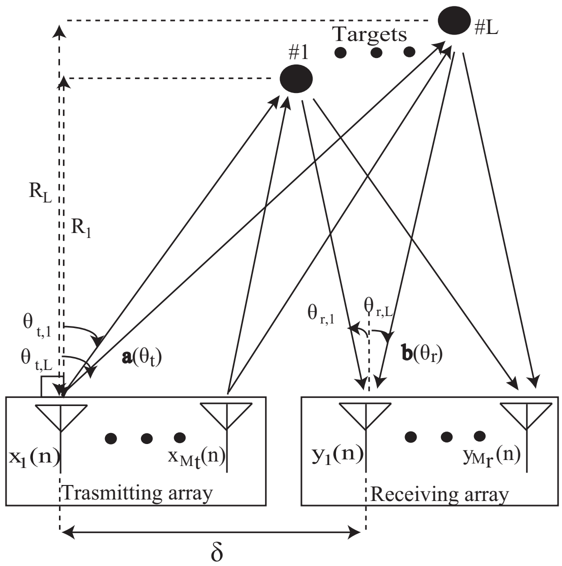

Figure 1: Analysis model of MIMO radar.

3. Estimation Algorithms

Location estimation is performed by using LS(Least-Square) method, Capon method, APES (Amplitude and Phase Estimation) method [2] and the MUSIC(MUltiple SIgnal Classification) algorithm [1]. The former three methods are of the beamforming type, and the last one is of the nulling type. The spectrum functions of LS, Capon, APES and MUSIC can be expressed respectively as follows [2]:

$$\beta_{LS} = \frac{\boldsymbol{b}^H(R_l,\theta_r)\boldsymbol{Y}\boldsymbol{X}^H\boldsymbol{a}^*(R_l,\theta_t)}{N\boldsymbol{b}^H(R_l,\theta_r)\boldsymbol{b}(R_l,\theta_r)\boldsymbol{a}^T(R_l,\theta_t)\boldsymbol{R}_{xx}\boldsymbol{a}^*(R_l,\theta_t)} \tag{9}$$

$$\beta_{Capon} = \frac{\boldsymbol{b}^H(R_l,\theta_r)\boldsymbol{R}_{yy}^{-1}\boldsymbol{Y}\boldsymbol{X}^H\boldsymbol{a}^*(R_l,\theta_t)}{N[\boldsymbol{b}^H(R_l,\theta_r)\boldsymbol{R}_{yy}^{-1}\boldsymbol{b}(R_l,\theta)][\boldsymbol{a}^T(R_l,\theta_t)\boldsymbol{R}_{xx}\boldsymbol{a}^*(R_l,\theta)]} \tag{10}$$

$$\beta_{APES} = \frac{\boldsymbol{b}^H(R_l,\theta)\boldsymbol{Q}^{-1}\boldsymbol{Y}\boldsymbol{X}^H\boldsymbol{a}^*(R_l,\theta)}{N[\boldsymbol{b}^H(R_l,\theta_r)\boldsymbol{Q}_1^{-1}\boldsymbol{b}(R_l,\theta_r)][\boldsymbol{a}^T(R_l,\theta_t)\boldsymbol{R}_{xx}\boldsymbol{a}^*(R_l,\theta_t)]} \tag{11}$$

$$\boldsymbol{Q} = \boldsymbol{R}_{yy} - \frac{\boldsymbol{Y}\boldsymbol{X}^H\boldsymbol{a}^*(R_l,\theta_t)\boldsymbol{a}^T(R_l,\theta_t)\boldsymbol{X}\boldsymbol{Y}^H}{N^2\boldsymbol{a}^T(R_l,\theta_t)\boldsymbol{R}_{xx}\boldsymbol{a}^*(R_l,\theta_t)} \tag{12}$$

$$P_{MU} = \frac{\boldsymbol{a}^T(R_l,\theta_t)\boldsymbol{a}^*(R_l,\theta_t)}{\boldsymbol{a}^T(R_l,\theta_t)\boldsymbol{E}_N\boldsymbol{E}_N^H\boldsymbol{a}^*(R_l,\theta_t)} \tag{13}$$

where $\boldsymbol{R}_{xx}$ and $\boldsymbol{R}_{yy}$ are the covariance matrices of the transmitted and received data, respectively, and $\boldsymbol{E}_N$ is the noise subspace matrix obtained from $\boldsymbol{H}^H\boldsymbol{H}$. Also, $(\cdot)^H$ denotes the complex conjugate transpose, $(\cdot)^*$ denotes the complex conjugate. When estimating the reception angle θ_r with MUSIC, we use $\boldsymbol{b}(R_l,\theta_{r,l})$ instead of $\boldsymbol{a}^*(R_l,\theta_{t,l})$ in eq.(13).

Here, the range R_l of the lth target has the following relationship:

$$R_l = \frac{\delta \cos\theta_{t,l} \cos\theta_{r,l}}{\sqrt{\cos^2\theta_{t,l} + \cos^2\theta_{r,l} - 2\cos\theta_{t,l}\cos\theta_{r,l}\cos(\theta_{t,l} - \theta_{r,l})}} \quad (14)$$

In the beamforming type methods, the peaks of spectrum correspond to the amplitude of targets, whereas the MUSIC requires another method to obtain the target amplitudes [2].

4. Performance Analysis by Computer Simulation

Under conditions shown in Tables 1 and 2, the computer simulation is carried out to clarify the characteristics of each method. First, it is assumed that all targets are at the same range R which is known in advance. When the three targets are closely spaced, the angle and β estimation results by the beamforming methods are shown in Fig.2, and the angle estimation result by MUSIC is shown in Fig. 3. The amplitudes of the three targets calculated from DOA estimates of MUSIC are (0.5000,1.0000,0.2500). From the results, it is confirmed that MUSIC provides high accuracy of estimation of both DOA and amplitudes compared with the three beamforming methods.

Next, under conditions shown in Table 3 where the range used in estimation is different from the exact value, a similar comparison between MUSIC and Capon methods is made. Figures 4 and 5 show the estimation results of MUSIC and Capon methods, respectively, and Table 4 shows the estimated ranges of the two methods by using eq.(14). It is found that the estimation accuracy of MUSIC is extremely high in the DOA and range estimation of targets.

Table 1: Common simulation conditions.

Array configuration	Uniform linear array of isotropic elements
Element spacing	0.5λ
Number of transmit antennas M_t	10
Number of receive antennas M_r	10
Number of targets L	3
Range to the targets R	all 100λ
Complex amplitude β	(0.5,1,0.25)
Number of samples N	64
Search interval in angle	0.05°
SNR	10dB

Table 2: Simulation conditions 1.

Distance between the reference antennas δ	0λ
Range used in DOA estimation	all 100λ
Transmission angles to the targets $\theta_t(=\theta_r)$	(10°,15°,20°)

Table 3: Simulation conditions 2.

Distance between the reference antennas δ	20λ
Transmission angle to the targets θ_t	(0°,30°,45°)
Range used in DOA estimation	all 90λ
Reception angle to the targets θ_r	(-11.3099°,20.6740°,38.6598°)

Table 4: Estimated ranges of targets in Fig.4 and 5.

Capon	$(89.9099\lambda, 90.0152\lambda, 90.0280\lambda)$
MUSIC	$(100.1419\lambda, 100.0924\lambda, 100.4208\lambda)$

5. Conclusion

In the MIMO radar, we have evaluated the characteristics of location estimation by the beamforming methods and MUSIC algorithm which is a popular nulling method. As a result of computer simulation, it is shown that the MUSIC algorithm reveals very high accuracy in the estimation of DOA, amplitudes and ranges of targets.

As the future work, we will try to carry out performance comparison including other algorithms and improve the algorithms to obtain higher estimation accuracy.

References

[1] N. Kikuma: *Adaptive Antenna Technology (in Japanese)* , Ohmsha, Inc., 2003.

[2] Jian Li and Petre Stoica: *MIMO Radar Signal Processing*, John Wiley & Sons, Inc., 2008.

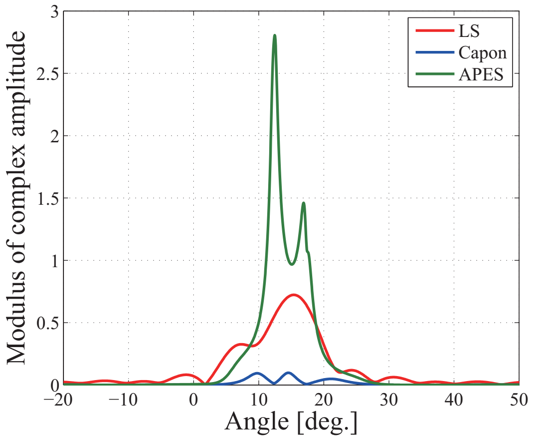

Figure 2: Spectrum of the beamforming methods under conditions in Table 2.

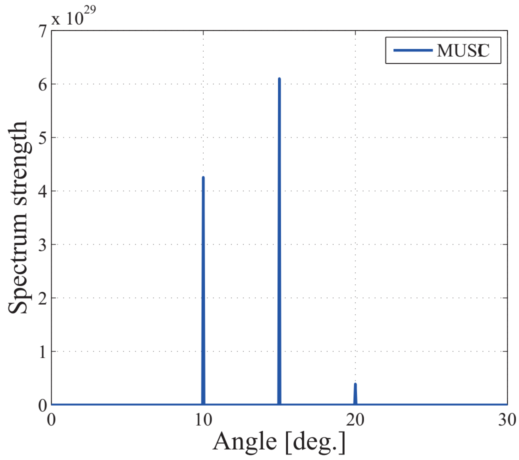

Figure 3: Spectrum of MUSIC under conditions in Table 2.

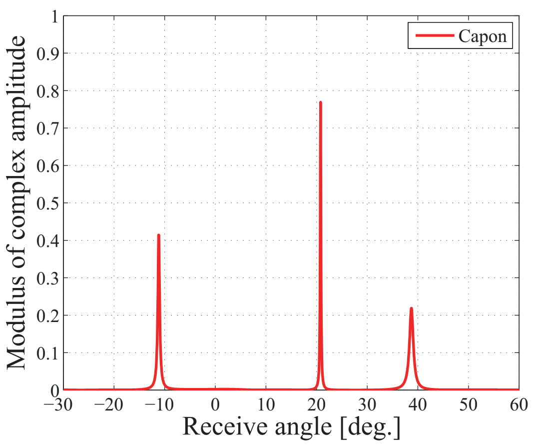

Figure 4: MUSIC spectrum in receiving array.

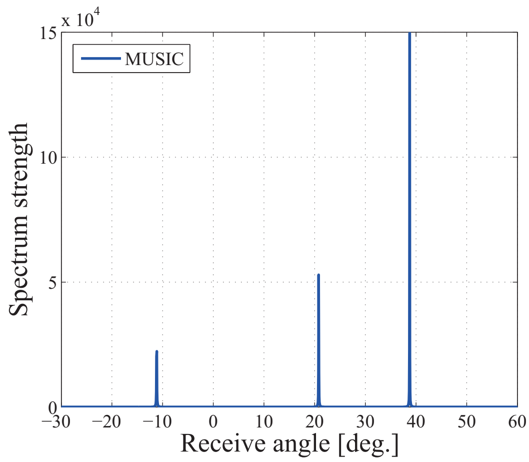

Figure 5: Capon spectrum in receiving array.